Development 135, 2807-2813 (2008) doi:10.1242/dev.022228

Origin and shaping of the laterality organ in zebrafish

Pablo Oteíza[1,*], Mathias Köppen[2,*], Miguel L. Concha[1,†] and Carl-Philipp Heisenberg[2]

Handedness of the vertebrate body plan critically depends on transient embryonic structures/organs that generate cilia-dependent leftward fluid flow within constrained extracellular environments. Although the function of ciliated organs in laterality determination has been extensively studied, how they are formed during embryogenesis is still poorly understood. Here we show that Kupffer's vesicle (KV), the zebrafish organ of laterality, arises from a surface epithelium previously thought to adopt exclusively extra-embryonic fates. Live multi-photon confocal imaging reveals that surface epithelial cells undergo Nodal/TGFβ signalling-dependent ingression at the dorsal germ ring margin prior to gastrulation, to give rise to dorsal forerunner cells (DFCs), the precursors of KV. DFCs then migrate attached to the overlying surface epithelium and rearrange into rosette-like epithelial structures at the end of gastrulation. During early somitogenesis, these epithelial rosettes coalesce into a single rosette that differentiates into the KV with a ciliated lumen at its apical centre. Our results provide novel insights into the morphogenetic transformations that shape the laterality organ in zebrafish and suggest a conserved progenitor role of the surface epithelium during laterality organ formation in vertebrates.

KEY WORDS: Enveloping layer, Epiboly, Organizer, Organogenesis, Kupffer's vesicle, Left-right asymmetry, Zebrafish

INTRODUCTION

A key step during the formation of the vertebrate body plan is the establishment of the left-right (LR) axis, which results in the characteristic asymmetric anatomy and positioning of the internal organs. Studies in several organisms have demonstrated that handedness of LR axis determination depends on the activity of a conserved embryonic ciliated structure (referred to as the organ of laterality), and involves a mechanism by which cilia beating generates a directed extracellular fluid flow (Nodal flow) that breaks the initial chemical and/or mechanical equilibrium of the embryo (McGrath et al., 2003; Nonaka et al., 1998; Tanaka et al., 2005).

Although the conservation and function of laterality organs are well established in vertebrates (Okada et al., 2005; Schweickert et al., 2007), comparatively little is known about their embryonic origin and the morphogenetic mechanisms leading to their formation. To obtain insights into these events, we analysed the formation of Kupffer's vesicle (KV), the zebrafish organ of laterality (Essner et al., 2005; Kramer-Zucker et al., 2005). KV is a transient organ proposed to arise from non-involuting, highly endocytic marginal blastomeres (deep NEM cells) that are positioned below surface-enveloping layer cells (EVL-NEM cells) at late blastula stage. Fate map studies have suggested that at the onset of gastrulation, deep NEM cells become displaced from the blastoderm margin to form a distinct group of dorsal forerunner cells (DFCs) (Cooper and D'Amico, 1996; D'Amico and Cooper, 1997; Melby et al., 1996). DFCs then move to the vegetal pole in close contact with the overlying EVL margin and become transformed into an epithelial vesicle (KV) that later produces a cilia-based flow within its interior lumen (Amack et al., 2007; Essner et al., 2005; Kramer-Zucker et al., 2005). During late somitogenesis, the vesicle collapses and DFCs become incorporated into notochord, somites and tail mesenchyme (Cooper and D'Amico, 1996). Despite these remarkably detailed studies, crucial questions remain concerning the cellular and molecular mechanisms that lead to DFC formation and the subsequent transformation of this cell group into a functional organ.

In this study, we demonstrate that DFCs are formed by ingression of surface epithelial cells at the dorsal margin of the zebrafish gastrula, and that Nodal/TGFβ signals are both required and sufficient to induce this process. We further show that, after ingression, a subset of cells within the DFC cluster retains its original polarisation through persistent apical contact with the overlying EVL. These pre-polarised cells serve as 'seeds' around which the remainder of DFCs assemble and epithelialise to form the mature KV. These findings point to a conserved mechanism of Nodal/TGFb-induced outer epithelium internalisation during laterality organ formation and demonstrate a novel mechanism by which external apicobasal polarity is propagated from the surface epithelium to an interior organ during vertebrate development.

MATERIALS AND METHODS

Zebrafish lines

The following zebrafish (*Danio rerio*) lines and alleles were used: wild-type TL, *Tg(sox17:GFP)* (Sakaguchi et al., 2006) and *Tg(β-actin:HRAS-EGFP)* (Cooper et al., 2005). Embryos were grown at 31°C unless otherwise indicated, manipulated in E3 zebrafish embryo medium or Danieau buffer, and staged according to morphology (Kimmel et al., 1995) and age [hours post-fertilisation (hpf)].

mRNA injections

For mRNA synthesis, pCS2+ expression vectors containing the cDNAs for different constructs were linearised with *Not*I and transcribed by SP6 mRNA polymerase as described (Montero et al., 2003). For mosaic expression, one marginal blastomere was injected at the 64-cell stage. mRNA amounts used for each experiment are given in the figure legends.

Immunohistochemistry

Embryos were fixed in 2% or 4% paraformaldehyde (PFA) and stained as described (Koppen et al., 2006). Stained embryos were mounted on agarose-coated dishes in phosphate buffered saline/0.5% Triton X-100 medium or embedded in 1% low-melting-point agarose. The following primary antibodies and dilutions were used: mouse anti-ZO-1 (Invitrogen, 1:200), rabbit anti-aPKC-ζ (Santa Cruz Biotechnology, 1:200) and mouse anti-

[1]Laboratory of Experimental Ontogeny, Program of Anatomy and Developmental Biology, Institute of Biomedical Sciences, University of Chile, Clasificador 7 – Correo 7, Santiago, Chile. [2]Max-Planck-Institute of Molecular Cell Biology and Genetics, Pfotenhauerstr.108, 01307 Dresden, Germany.

*These authors contributed equally to this work
†Author for correspondence (e-mail: mconcha@med.uchile.cl)

Accepted 19 June 2008

acetylated α-tubulin (Sigma, 1:400). Samples were imaged on a Zeiss LSM META confocal microscope using an Achroplan 40×/0.8 W dipping objective or a Plan-Apochromat 40×/1.2 W objective.

Live imaging

Embryos from *Tg(sox17:GFP)* and *Tg(β-actin:HRAS-EGFP)* in crosses or crosses between both lines were manually dechorionated and mounted in 0.5% low-melting-point agarose just prior to imaging. Time-lapse, multiple focal plane (4D) microscopy was then performed at 22°C or 28°C on a BioRad Radiance 2000 multi-photon or a Zeiss LSM META confocal system. Movies were processed using Volocity (Improvision) and ImageJ (http://rsb.info.nih.gov/ij/) software.

Image quantification

Lumen volume analysis was performed by generating 3D renderings of anti-aPKC-ζ staining using Volocity software. KV cilia length measurements were performed on *z*-projections of dorsal confocal stacks of *Tg(sox17:GFP)* embryos stained with anti-acetylated α-tubulin using ImageJ software. The number of DFCs during epiboly was determined using Imaris software (Bitplane), employing the spot recognition function to count cell nuclei of *sox17*:*GFP*-expressing DFC clusters.

RESULTS

Dorsal forerunner cell formation, polarisation and migration

To address the mechanism that leads to the formation of the DFCs, we performed time-lapse multi-photon confocal imaging of sphere-stage zebrafish embryos (4 hpf) expressing the membrane marker *Tg(β-actin:HRAS-EGFP)*. At this stage, the blastoderm consists of two main tissues: an outer epithelial monolayer referred to as the enveloping layer (EVL), and the deep cells that make up the embryo proper. Both tissues then undergo a vegetal movement in order to enwrap the yolk cell in a process known as epiboly (Kimmel et al., 1995) (see Fig. 1M for illustration).

As expected, we found that at the sphere stage, DFCs were not yet discernible at the future dorsal side of the embryo. Instead, we observed dorsal surface epithelial (DSE) cells that were in direct contact with the yolk syncytial layer and exhibited filopodia-like protrusions at their leading edge (Fig. 1A,G,J,M). Strikingly, we found that during subsequent development, a subset of marginal and submarginal DSE cells internalise through a process of ingression

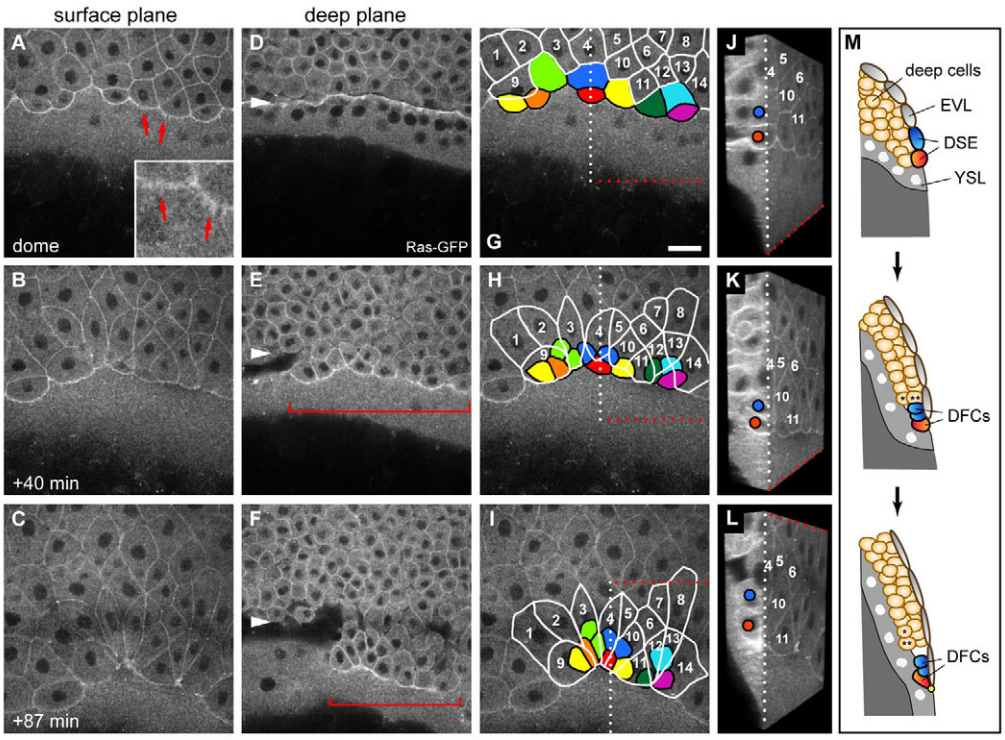

Fig. 1. Dorsal forerunner cells are derived from dorsal surface epithelial cells. Images of a time-lapse multi-photon confocal movie of a zebrafish embryo expressing *Tg(β-actin:HRAS-EGFP)*. Dorsal view with animal pole to the top. (**A-C**) Single focal planes through the surface of the embryo at early dome stage (~4.2 hpf) and subsequent time points show the progression of dorsal surface epithelial (DSE) cells towards the vegetal pole. Some marginal DSE cells form filopodia-like protrusions at their leading edge (arrows and inset in A). (**D-F**) Images of the deep cell layer at equivalent time points to A-C, with the deep cell margin marked with arrowheads. DFCs (brackets) become visible directly in front of the deep cell margin shortly after the dome stage (E) and then move progressively away from the margin (F). (**G-I**) Fate mapping of DSE cells shows that nine of these cells at or close to the margin (coloured), but no deep cells, become converted into DFCs. Cells remaining within the enveloping layer (EVL) are outlined in white and traced by number. The same principal finding was made in all five embryos analysed by live imaging. The DSE-to-DFC conversion occurs as the DSE cells round up and become covered by the trailing EVL cells that form the new EVL margin. During this process, two of these cells (light green and dark blue) can be seen to divide once (H,I). During vegetal movement, both EVL cells and DFCs converge to the dorsal side. (**J-L**) Three-dimensional rendering and cutting of the image stacks along the dotted lines shown in G-I allows simultaneous display of the *xy* and *yz* axes, and reveals the repositioning of red and dark-blue DSE cells below the tissue. (**M**) Schematic representation of DSE-to-DFC conversion and deep cell internalisation as observed in the live recording. Two DSE cells, depicting the red and dark-blue DSE cells in the movie, become positioned beneath the EVL to become DFCs. The blue cell had divided immediately prior to internalisation. The attachment point linking DFCs to the EVL is shown as a yellow spot. Two deep cells (asterisks) are shown to undergo internalisation to form hypoblast. Scale bar: 30 μm.

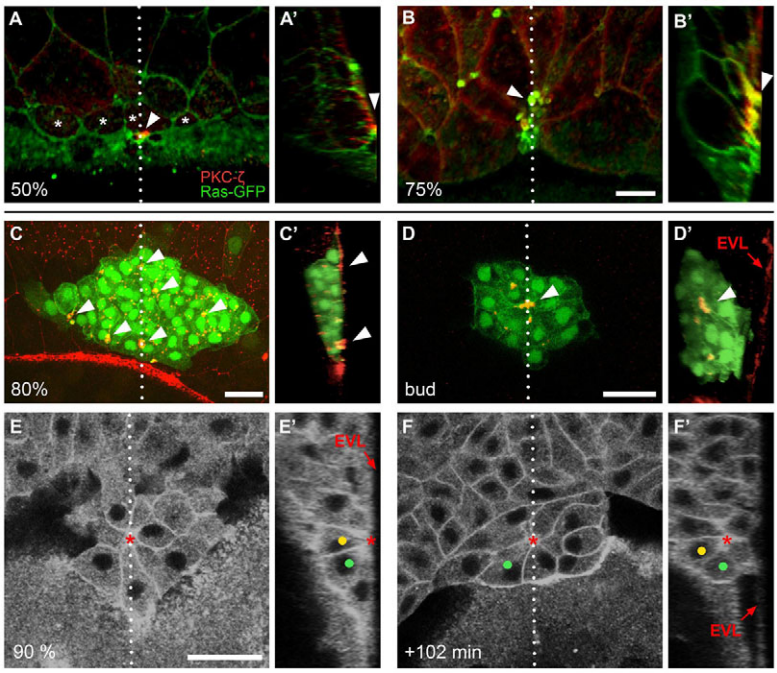

Fig. 2. Apical attachment of the dorsal forerunner cell cluster to the enveloping layer and subsequent detachment to form a cellular rosette during gastrulation. (**A-B′**) Confocal images of *Tg(β-actin:HRAS-EGFP)* zebrafish embryos immunolabelled with an anti-aPKC-ζ antibody. GFP (green) and aPKC-ζ (red) channels are merged. Single dorsal focal planes (A,B) and sagittal sections at the position of the dotted line (A′,B′; embryo surface to the right) are shown. Animal pole is to the top. A surface plane through an embryo at 50% epiboly shows that presumptive DFCs (asterisks) are partially positioned underneath the EVL (A). Clear enrichment of aPKC-ζ is found at the contact point between one of the DFCs and the overlying EVL (A,A′; arrowheads). At 75% epiboly, the EVL completely covers the DFCs (B). A sagittal section shows bottle-shaped DFCs with strong aPKC-ζ enrichment at the contact points with the EVL (B′; arrowheads). (**C-D′**) Confocal images of *Tg(sox17:GFP)*-expressing embryos immunolabelled with an anti-ZO-1 antibody. GFP (green) and anti-ZO-1 (red) channels are merged. At 80% epiboly, DFCs form a compact cluster that is in contact with the interior surface of the EVL close to the margin. Anti-ZO-1 signal is enriched at contact points (arrowheads) between DFCs and the overlying EVL (dorsal *z*-projection is shown in C; sagittal section at the position of the dotted line in C′). At the bud stage, a ZO-1-rich focal point (arrowhead) is seen at the centre of the DFC cluster (single focal plane is shown in D; sagittal section at the position of the dotted line in D′). The cluster is disconnected from the overlying EVL. (**E-F′**) Images of a time-lapse multi-photon confocal movie of a *Tg(β-actin:HRAS-EGFP)* embryo, showing DFC cluster arrangement and tracing of two DFCs (green and yellow dots). Single dorsal focal planes (E,F) and sagittal sections at the position of the dotted line (E′,F′) are shown. At 90% epiboly, several bottle-shaped DFCs are attached to the overlying EVL via a single focal point (asterisk), including the two marked cells (E,E′; arrow indicates the position of the EVL). At +102 minutes, the marked cells have internalised and become part of a DFC rosette that is arranged around an interior focal point (F,F′; focal point marked by asterisk). Scale bars: 30 μm.

beneath the surface epithelium (Fig. 1; see Movies 1 and 2 in the supplementary material; data not shown). Ingression occurred as trailing cells of the EVL moved over the DSE cells, displacing them beneath the surface. Once ingressed, DSE cells were clearly recognisable as DFCs by their position below the EVL margin and ahead of the deep cell margin. We will therefore refer to these newly ingressed cells as DFCs. These cells most likely correspond to the previously described deep NEM cells (Cooper and D'Amico, 1996; D'Amico and Cooper, 1997). However, whereas deep NEM cells were observed to lie within the dorsal blastoderm margin, we found newly ingressed DSE cells to be positioned ahead of the deep cell margin. This discrepancy is most likely due to the different labelling and imaging methods used to identify DFCs. Together, we conclude that DFCs form via the ingression of marginal and submarginal DSE cells beneath the surface epithelium.

Importantly, we observed no incidences of deep cell conversion into DFCs (n=5 embryos; Fig. 1G-I; see Movies 1 and 2 in the supplementary material; data not shown). Moreover, the analysis of surface epithelial morphogenesis in lateral or ventral regions of the embryo revealed only very sporadic cell ingression (1/115 cells in 10 embryos; see Movie 3 in the supplementary material), indicating that coordinated ingression behaviour is restricted to DSE cells.

DSE cell ingression was often immediately preceded by a cell division (Fig. 1G-I,M; see Movie 2 in the supplementary material). Typically, the division occurred in the plane of the epithelium, giving rise to two ingressing cells. However, in younger embryos (around the 'high' stage, 3.3 hpf), we frequently observed delaminating divisions of DSE cells, which gave rise to a DSE cell and a deep cell. We observed that in a few instances, the newly formed DSE cell became a DFC, while the second daughter cell exclusively became a deep cell (see Fig. S1 and Movie 4 in the supplementary material). This finding is surprising, as previous analysis of cell division patterns of the zebrafish blastula had suggested that a DSE cell resulting from a delaminating division is committed to the EVL fate (Kane et al., 1992). Together, we conclude that the type of DSE cell division does not strictly correlate with EVL versus DFC fate.

DFC formation took place concurrently with the onset of embryonic epiboly, during which marginal deep cells, marginal EVL cells and DFCs all advance towards the vegetal pole (Cooper and D'Amico, 1996; Melby et al., 1996). We found that the conversion of DSE cells into DFCs consistently completed by 50% epiboly, immediately prior to the formation of the embryonic organizer (shield). As epiboly progressed, the DFC group became increasingly separated from the dorsal marginal deep cells and remained in direct contact with the advancing dorsal EVL margin (Fig. 1G-I,M) (D'Amico and Cooper, 1997). Furthermore, the number of DFCs increased between shield stage and 80% epiboly from 31±9 (n=16 embryos, mean±s.d.) to 50±11 (n=9), as determined using a *Tg(sox17:GFP)* transgenic line (see below). This increase is likely to be due primarily to cell division within the cell cluster, based on our analysis of time-lapse movies (data not shown). These numbers are higher than those determined previously (Cooper and D'Amico, 1996), probably because of the different methodologies applied to identify DFCs (see Materials and methods).

Ongoing with vegetal DFC progression, DFCs rapidly converged to the dorsal side by intercalating between each other, thereby transforming the initially wide array of cells into a more compact and oval-shaped cluster by about 80% epiboly (Fig. 1D-I; see Movie 5 and Figs S2 and S3 in the supplementary material). This

convergence was notably mirrored by dorsal convergence of the overlying dorsal marginal EVL cells (Fig. 1A-C,G-I). Strikingly, a subset of DFCs became increasingly bottle-shaped during epiboly and remained persistently linked to the dorsal EVL margin via attachment points that were enriched for the tight-junction components ZO-1 (Tjp1 – ZFIN) and protein kinase C zeta (aPKC-ζ; Prkcz – ZFIN) (Fig. 2A-B′ and data not shown). By contrast, the remainder of cells in the cluster appeared unpolarised, forming dynamic cell protrusions without a preferential orientation (see Movie 5 and Fig. S3 in the supplementary material). This suggests that tight-junction based DFC-EVL attachment couples the vegetal movement and convergence of both tissues. This finding is consistent with previous analyses suggesting that the movement of DFCs and of the EVL are coupled via physical tissue linkage (D'Amico and Cooper, 1997; Solnica-Krezel et al., 1996).

DFC epithelialisation and transformation into KV

To characterise the cellular events that transform the relatively unstructured DFC cluster into a highly organised vesicle after completion of embryonic epiboly, we made use of a transgenic fish line that strongly expresses GFP in DFCs via the *sox17* promoter (Sakaguchi et al., 2006). Consistent with the above results, we found that multiple subgroups of bottle-shaped DFCs were attached to overlying dorsal marginal EVL cells via ZO-1-rich subcellular structures at 80% epiboly (Fig. 2C,C′). After reaching the vegetal pole during the final phase of epiboly, the cluster became separated from the overlying dorsal marginal EVL cells, most likely owing to dorsal marginal deep cells moving between the two tissues during the vegetal sealing of the embryo (Fig. 2D,D′; see Fig. S2 in the supplementary material). Using both live imaging and immunolabelling, we found that during this separation the apices of bottle-shaped DFCs turned towards the inside of the cluster and generated multiple three-dimensional rosette structures around ZO-1-rich apical focal points (Fig. 2D,D′,F,F′; see Movie 6 in the supplementary material). At the same time, the DFC cluster became increasingly compact and acquired the shape of a flattened sphere (Fig. 2C-D′; see Figs S2 and S3 in the supplementary material).

The separation of the DFC cluster from dorsal marginal EVL cells and its rearrangement into rosettes was quickly followed by the formation of an interior vesicle lumen (Fig. 3A-C; see Movie 7 in the supplementary material). This occurred as the initially widely spaced apical focal points within the cluster coalesced into a dense network around which cells arranged into a single large rosette structure, incorporating previously unpolarised DFCs. During these rearrangements, small extracellular lumina typically formed at multiple apical focal points (Fig. 3A,B,D,E,G,H) and rapidly fused into a single ZO-1-lined lumen (Fig. 3C,F,I). Lumen volume then increased approximately 12-fold between the 1-somite and 4-somite stages (see Fig. S4 in the supplementary material). Live imaging of DFCs expressing GFP revealed that cytoplasmic, vacuole-like structures fused with the apical membrane domain as the lumen formed, suggesting that apical vacuole fusion contributes to apical membrane expansion and lumen growth (see Movie 8 in the supplementary material). Interestingly, we found that lumen formation was directly coupled to ciliogenesis. Small, tubulin-rich cilia were first detected at the onset of lumen initiation, when the lumen-facing membrane domain of polarised DFCs started developing cilia (Fig. 3J-L). Lumen volume and cilia length continuously increased during KV maturation (between bud and 4-somite stage), while cilia number remained essentially constant (see Fig. S4 in the supplementary material). This suggests that no

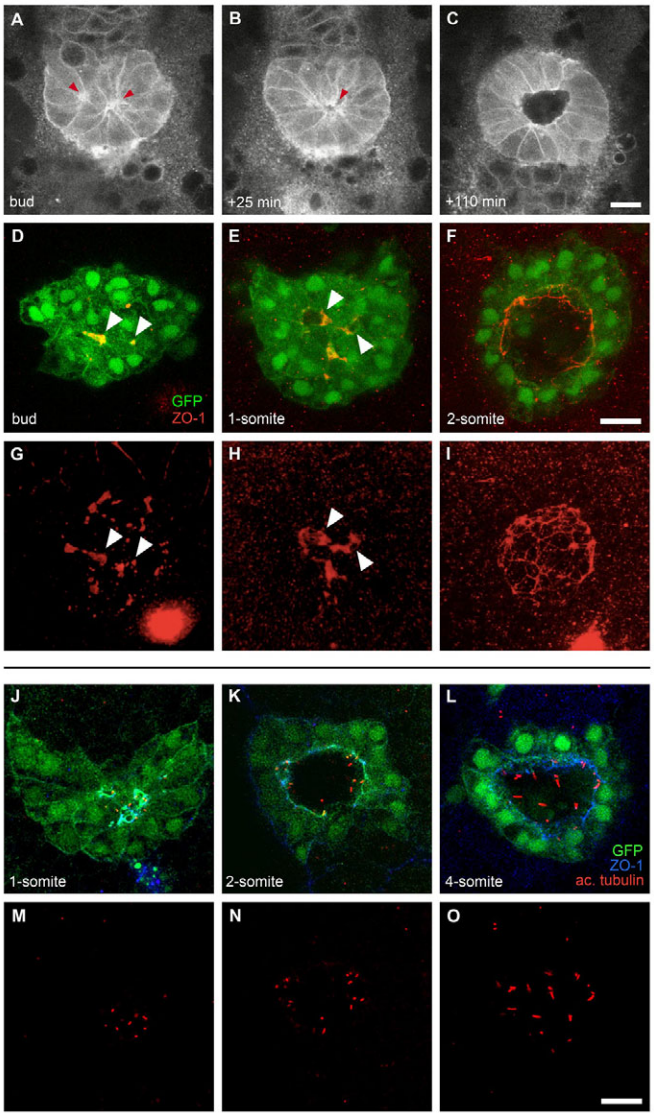

Fig. 3. Lumen and cilia formation in Kupffer's vesicle. (**A-C**) Images of a time-lapse multi-photon confocal movie of a zebrafish embryo expressing *Tg(β-actin:HRAS-EGFP;sox17:GFP)*. Single focal planes at the interior of the DFC cluster are shown at the bud stage and subsequent time points, as indicated. Anterior is to the top. At the bud stage, bottle-shaped DFCs are arranged around two focal points (A, arrowheads). Shortly after, these focal points have coalesced into a single focal point (B, arrowhead) from which a single lumen forms (C). (**D-I**) Confocal images of *Tg(sox17:GFP)*-expressing embryos immunolabelled with an anti-ZO-1 antibody. GFP, green; anti-ZO-1, red. Single focal planes at the interior of the DFC cluster (D-F) and 3D renderings of the anti-ZO-1 labelling (G-I) are shown. Arrowheads mark equivalent structures in single focal planes and renderings. At the bud stage, multiple, widely spread ZO-1-rich accumulations are found in the interior of the DFC cluster (D,G). At the 1-somite stage, ZO-1 clusters are more connected and condensed, and small lumina are observed (E,H). At the 2-somite stage, a single, large lumen delineated by ZO-1 is observed inside the cluster (F,I). (**J-O**) Confocal images of *Tg(sox17:GFP)*-expressing embryos (green) double labelled with anti-ZO-1 (blue) and anti-acetylated α-tubulin (red) antibodies. Single focal planes are shown for merged (J-L) and single (M-O) channels. At the 1-somite stage, DFCs are positioned around multiple small lumina delineated by ZO-1, in which short, tubulin-rich cilia are observed (J,M). Between the 2- and 4-somite stages, a single, expanding lumen is observed (K,L), which contains cilia that are increasing in length (N,O). Scale bars: 30 μm.

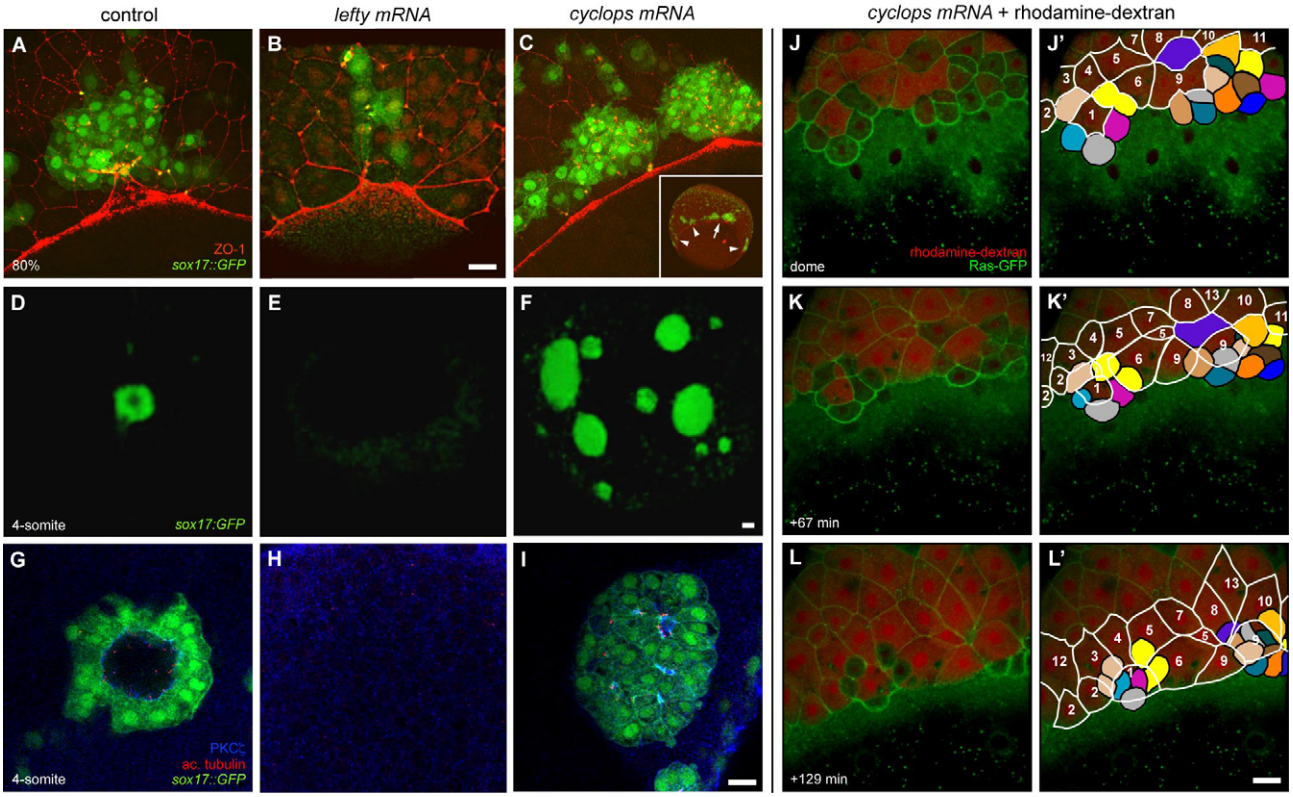

Fig. 4. Nodal/TGFβ signalling regulates dorsal forerunner cell formation in a non-cell autonomous manner. (**A-C**) Confocal images of 75% epiboly *Tg(sox17:GFP)*-expressing zebrafish embryos immunolabelled with an anti-ZO-1 antibody. *z*-projections with GFP in green and anti-ZO-1 in red are shown. In a control embryo, DFCs form a compact cluster in contact with the EVL margin (A). A sibling embryo of equivalent age injected with 100 pg of *lefty*-encoding mRNA shows a markedly reduced number of DFCs (B). By contrast, a sibling embryo injected with 100 pg of *cyclops*-encoding mRNA shows a clear increase in DFC number (C). A low-magnification image of the same embryo (inset in C) shows the appearance of multiple, widely spaced DFC clusters positioned all along the EVL margin (the main cluster is indicated by an arrow in the inset, additional clusters by arrowheads). (**D-I**) Confocal images of 4-somite stage *Tg(sox17:GFP)*-expressing embryos immunolabelled for aPKC-ζ and acetylated tubulin. Vegetal views of 3D-projections of low-magnification images showing GFP in green (D-F) and single focal planes of high-magnification images showing GFP in green, aPKC-ζ in blue and acetylated tubulin in red (G-I). In a control embryo, DFCs form a single, oval-shaped DFC cluster with a ciliated interior lumen (D,G). In a *lefty*-mRNA-injected embryo of equivalent age, no DFCs are observed (E,H), whereas a *cyclops*-mRNA-injected embryo displays multiple, abnormally large DFC clusters with significantly smaller, ciliated lumina (F,I). (**J-L'**) Images from a time-lapse confocal movie of a *Tg(β-actin:HRAS-EGFP)* embryo co-injected with 50 pg of *cyclops* mRNA and rhodamine-dextran into a single marginal blastomere at the 64-cell stage. The animal pole is to the top. Three-dimensional projections of the embryo at the dome stage (~4.2 hpf) and subsequent time points are shown (J-L). Fate mapping of surface epithelial cells shows that ten rhodamine-negative cells and five cells with low rhodamine signal (coloured) become displaced below the EVL margin (J'-L'). By contrast, all cells remaining at the embryonic surface (cells outlined in white and traced by number) are rhodamine-positive. Scale bars: 70 μm in D-F; 20 μm in A-C,G-L'.

additional cilia-forming cells are recruited to the cluster during lumen formation and expansion. Together, these observations suggest that initial DFC polarisation is established during epiboly and contributes to the subsequent formation of rosette structures by a subset of polarised DFCs. Later epithelial differentiation to form KV involves concurrent lumen formation and ciliogenesis.

The role of Nodal signalling during DFC formation

Our dynamic analysis of DFC formation revealed a principal mechanism that resembles the formation of the internal germ layers, which are formed through cell internalisation beneath the future ectoderm. Numerous studies have demonstrated that the Nodal signalling pathway acts as a key regulator of this process (reviewed by Schier and Talbot, 2005). Importantly, recent reports have shown that DFC number increases or decreases in response to enhanced or reduced Nodal signalling, respectively (Choi et al., 2007). In agreement with this, we observed that overexpression of the Nodal antagonist Lefty strongly decreased the DFC number (Fig. 4B,E,H). In addition, maternal-zygotic *one-eyed pinhead* mutants, which are defective for Nodal signalling, completely lacked recognisable DFCs at 80% epiboly (data not shown). Together, this strongly suggests that Nodal signalling is required for surface cell internalisation to generate DFCs.

To test whether Nodal signalling acts instructively during DFC formation, we performed gain-of-function experiments by overexpressing the Nodal signalling ligand Cyclops (Cyc; Ndr2 – ZFIN). Strikingly, we observed that numerous DFC clusters were generated from DSE cells along the whole circumference of the embryo (Fig. 4C). A major dorsal cluster was typically observed that showed increased DFC number at 80% epiboly (104±50, n=5 embryos, mean±s.d.) compared with uninjected controls (50±11, n=9). The enlarged DFC clusters were attached to the EVL margin via apical cell domains, similar to in controls (Fig. 4A,C). Multiple DFC clusters were also observed at the bud stage and early somite

stages. These clusters typically contained the characteristic interior apical focal points of controls and underwent partial lumen formation (Fig. 4F,I, and data not shown). These results indicate that enhanced Nodal signalling is sufficient to induce ectopic DFC clusters that undergo partially normal morphogenetic transformation.

To gain insight into the dynamics of ectopic DFC formation in Nodal-overexpressing embryos, we performed time-lapse confocal imaging of *Tg(β-actin:HRAS-EGFP)* embryos co-injected with *cyc* mRNA and fluorescently labelled dextran (to identify *cyc*-expressing cells). Importantly, we found that in these embryos, DFCs formed via the same principal mechanism observed in controls (see Fig. 1). Namely, surface epithelial cells located at the Cyc-overexpressing side of the embryo became transformed into DFCs-like cells through their displacement beneath the EVL sheet after sphere stage (Fig. 4J-L′; see Movie 9 in the supplementary material). In addition, we found this behaviour predominantly in the dextran-negative cells (n=3 movies), suggesting that Cyc induces cell ingression in a non-cell-autonomous manner. In summary, our findings indicate that DFC formation through ingression of surface epithelial cells is controlled by Nodal signalling, which plays both instructive and permissive roles in this process.

DISCUSSION

In this study, we have investigated the mechanisms leading to the formation of DFCs in the zebrafish embryo, and the subsequent transformation of this group of cells into KV. Our findings reveal that DFCs are formed through the ingression movement of a subset of surface epithelial cells on the dorsal side of the embryo (DSE cells). Ingression is initiated after sphere stage (midway through the blastula period, 4 hpf) and occurs progressively until 50% epiboly [the onset of gastrulation, 5.3 hpf; see Kimmel et al. (Kimmel et al., 1995) for embryonic stages]. Notably, this cell behaviour predominantly occurs in a region of the dorsal blastoderm margin that is homologous to the organizer epithelium of *Xenopus* (Cooper and Virta, 2007; Shih and Keller, 1992). This suggests that DFCs are formed through a previously unrecognised process of organizer epithelium ingression in zebrafish. Interestingly, this organizer epithelial cell ingression represents the earliest morphogenetic cell behaviour specifically linked to the ontogeny of the organizer region in zebrafish. Furthermore, it adds to the notion that the organizer region can be subdivided into domains of distinct morphogenetic behaviours that generate distinct organ rudiments such as KV, prechordal plate and notochord (Coopers and Virta, 2007; Montero et al., 2003). Together, these findings provide novel insights into cell lineage decisions and morphogenesis of the organizer region at the onset of zebrafish gastrulation.

Previous analysis has suggested that KV formation involves a mesenchymal-to-epithelial transition of the DFC cluster (Amack et al., 2007). Here we show that vesicle formation involves an early phase in which epithelial surface cells convert into deep DFCs with mesenchymal behaviour, followed by a phase of re-epithelialisation that transforms the DFC cluster into a ciliated epithelial vesicle. Intriguingly, a subset of polarised DFCs persistently retains epithelial properties throughout the organogenetic process. These DFCs initially form apical contacts with the EVL, which is likely to facilitate their vegetal movement. Subsequently, the polarity of these cells is maintained as they become internalised and form the ‘seeds’ around which the remaining mesenchymal DFCs assemble into polarised rosettes. This observation suggests that epithelial polarity is not initiated de novo within the DFC cluster, but is instead derived from the apicobasal polarity of the surface epithelium. Thus, the initial apicobasal polarity of an embryonic surface tissue provides the polarising cue that underlies the formation of a polarised interior organ. These findings provide important new insights into embryological mechanisms underlying the initiation and propagation of epithelial polarity.

Our finding that KV derives from an embryonic surface epithelium offers new perspectives concerning the evolutionary conservation of laterality organ formation in vertebrates. Similar to KV in zebrafish, the amphibian laterality organ (the gastrocoel roof plate) is a transient ciliated epithelium that forms through internalisation of surface epithelium of the dorsal organizer region (Schweickert et al., 2007; Shook et al., 2004). Moreover, the precursors of the mammalian organ of laterality (the posterior notochordal plate) also appear to be derived from the epithelial epiblast (Blum et al., 2007; Hirokawa et al., 2006; Kinder et al., 2001). However, whereas in *Xenopus*, where organizer surface epithelial cells internalise through involution, in zebrafish they undergo ingression, suggesting that the cytomechanics of organizer surface epithelium internalisation has evolved differently along phylogenetic lineages (reviewed by Cooper and Virta, 2007).

Our evidence for a role of Nodal signalling during organizer epithelium internalisation and DFC specification additionally suggests that the conservation of vertebrate laterality organ formation also extends to the molecular level. In *Xenopus*, specification of the dorsal organizer epithelium is dependent on Nodal signals produced by the vegetal endoderm (reviewed by Shook et al., 2004). Moreover, specification of the mammalian anterior head process precursors, a group of cells that contributes to the notochordal plate, also requires high levels of Nodal signalling (Vincent et al., 2003; Yamanaka et al., 2007). Together, this strongly points to a conserved role for Nodal signalling during internalisation of outer epithelia, which is likely to be the initial step in vertebrate laterality organ formation. Further studies analysing vertebrate species other than zebrafish will be needed to fully elucidate the conserved cellular and molecular mechanisms by which vertebrate embryos acquired a cilia-dependent, Nodal flow-based strategy to control the handedness of their body plan.

We are particularly grateful to J. Stühmer, M. Krieg, D. Müller, S. Preibisch and P. Tomancak for contributing data to earlier versions of this manuscript; to P. Stockinger for suggesting the use of *Tg(sox17:GFP)* fish; to J. Peychl and J. Sanderson for microscopy advice; to E. Lehmann, J. Hückmann, G. Junghanns and D. Silva for fish-care; to Y. Arboleda, S. Schneider, R. Pérez and A. Catenaccio for technical help; and to L. Rohde, J. Geiger and M. Tada for valuable advice on earlier versions of the manuscript. This work was supported by grants from the DFG, MPG and EU to C.-P.H., from the PBCT (ACT47), CONICYT/DAAD (2003-4-124), MIDEPLAN (ICM P04-068-F), HHMI (INTNL55005940) and EU (FP6-NEST-PATH EDCBNL) to M.L.C., and from the Proyecto Mecesup UCH0306 and DAAD to P.O.

Supplementary material

Supplementary material for this article is available at
http://dev.biologists.org/cgi/content/full/135/16/2807/DC1

References

Amack, J. D., Wang, X. and Yost, H. J. (2007). Two T-box genes play independent and cooperative roles to regulate morphogenesis of ciliated Kupffer’s vesicle in zebrafish. *Dev. Biol.* **310**, 196-210.

Blum, M., Andre, P., Muders, K., Schweickert, A., Fischer, A., Bitzer, E., Bogusch, S., Beyer, T., van Straaten, H. W. and Viebahn, C. (2007). Ciliation and gene expression distinguish between node and posterior notochord in the mammalian embryo. *Differentiation* **75**, 133-146.

Choi, W. Y., Giraldez, A. J. and Schier, A. F. (2007). Target protectors reveal dampening and balancing of Nodal agonist and antagonist by miR-430. *Science* **318**, 271-274.

Cooper, M. S. and D’Amico, L. A. (1996). A cluster of noninvoluting endocytic cells at the margin of the zebrafish blastoderm marks the site of embryonic shield formation. *Dev. Biol.* **180**, 184-198.

Cooper, M. S. and Virta, V. C. (2007). Evolution of gastrulation in the ray-finned (actinopterygian) fishes. *J. Exp. Zool. B Mol. Dev. Evol.* **308**, 591-608.
Cooper, M. S., Szeto, D. P., Sommers-Herivel, G., Topczewski, J., Solnica-Krezel, L., Kang, H. C., Johnson, I. and Kimelman, D. (2005). Visualizing morphogenesis in transgenic zebrafish embryos using BODIPY TR methyl ester dye as a vital counterstain for GFP. *Dev. Dyn.* **232**, 359-368.
D'Amico, L. A. and Cooper, M. S. (1997). Spatially distinct domains of cell behavior in the zebrafish organizer region. *Biochem. Cell Biol.* **75**, 563-577.
Essner, J. J., Amack, J. D., Nyholm, M. K., Harris, E. B. and Yost, H. J. (2005). Kupffer's vesicle is a ciliated organ of asymmetry in the zebrafish embryo that initiates left-right development of the brain, heart and gut. *Development* **132**, 1247-1260.
Hirokawa, N., Tanaka, Y., Okada, Y. and Takeda, S. (2006). Nodal flow and the generation of left-right asymmetry. *Cell* **125**, 33-45.
Kane, D. A., Warga, R. M. and Kimmel, C. B. (1992). Mitotic domains in the early embryo of the zebrafish. *Nature* **360**, 735-737.
Kimmel, C. B., Ballard, W. W., Kimmel, S. R., Ullmann, B. and Schilling, T. F. (1995). Stages of embryonic development of the zebrafish. *Dev. Dyn.* **203**, 253-310.
Kinder, S. J., Tsang, T. E., Wakamiya, M., Sasaki, H., Behringer, R. R., Nagy, A. and Tam, P. P. (2001). The organizer of the mouse gastrula is composed of a dynamic population of progenitor cells for the axial mesoderm. *Development* **128**, 3623-3634.
Koppen, M., Fernandez, B. G., Carvalho, L., Jacinto, A. and Heisenberg, C. P. (2006). Coordinated cell-shape changes control epithelial movement in zebrafish and Drosophila. *Development* **133**, 2671-2681.
Kramer-Zucker, A. G., Olale, F., Haycraft, C. J., Yoder, B. K., Schier, A. F. and Drummond, I. A. (2005). Cilia-driven fluid flow in the zebrafish pronephros, brain and Kupffer's vesicle is required for normal organogenesis. *Development* **132**, 1907-1921.
McGrath, J., Somlo, S., Makova, S., Tian, X. and Brueckner, M. (2003). Two populations of node monocilia initiate left-right asymmetry in the mouse. *Cell* **114**, 61-73.
Melby, A. E., Warga, R. M. and Kimmel, C. B. (1996). Specification of cell fates at the dorsal margin of the zebrafish gastrula. *Development* **122**, 2225-2237.
Montero, J. A., Kilian, B., Chan, J., Bayliss, P. E. and Heisenberg, C. P. (2003). Phosphoinositide 3-kinase is required for process outgrowth and cell polarization of gastrulating mesendodermal cells. *Curr. Biol.* **13**, 1279-1289.
Nonaka, S., Tanaka, Y., Okada, Y., Takeda, S., Harada, A., Kanai, Y., Kido, M. and Hirokawa, N. (1998). Randomization of left-right asymmetry due to loss of nodal cilia generating leftward flow of extraembryonic fluid in mice lacking KIF3B motor protein. *Cell* **95**, 829-837.
Okada, Y., Takeda, S., Tanaka, Y., Belmonte, J. C. and Hirokawa, N. (2005). Mechanism of nodal flow: a conserved symmetry breaking event in left-right axis determination. *Cell* **121**, 633-644.
Sakaguchi, T., Kikuchi, Y., Kuroiwa, A., Takeda, H. and Stainier, D. Y. (2006). The yolk syncytial layer regulates myocardial migration by influencing extracellular matrix assembly in zebrafish. *Development* **133**, 4063-4072.
Schier, A. F. and Talbot, W. S. (2005). Molecular genetics of axis formation in zebrafish. *Annu. Rev. Genet.* **39**, 561-613.
Schweickert, A., Weber, T., Beyer, T., Vick, P., Bogusch, S., Feistel, K. and Blum, M. (2007). Cilia-driven leftward flow determines laterality in Xenopus. *Curr. Biol.* **17**, 60-66.
Shih, J. and Keller, R. (1992). The epithelium of the dorsal marginal zone of Xenopus has organizer properties. *Development* **116**, 887-899.
Shook, D. R., Majer, C. and Keller, R. (2004). Pattern and morphogenesis of presumptive superficial mesoderm in two closely related species, Xenopus laevis and Xenopus tropicalis. *Dev. Biol.* **270**, 163-185.
Solnica-Krezel, L., Stemple, D. L., Mountcastle-Shah, E., Rangini, Z., Neuhauss, S. C., Malicki, J., Schier, A. F., Stainier, D. Y., Zwartkruis, F., Abdelilah, S. et al. (1996). Mutations affecting cell fates and cellular rearrangements during gastrulation in zebrafish. *Development* **123**, 67-80.
Tanaka, Y., Okada, Y. and Hirokawa, N. (2005). FGF-induced vesicular release of Sonic hedgehog and retinoic acid in leftward nodal flow is critical for left-right determination. *Nature* **435**, 172-177.
Vincent, S. D., Dunn, N. R., Hayashi, S., Norris, D. P. and Robertson, E. J. (2003). Cell fate decisions within the mouse organizer are governed by graded Nodal signals. *Genes Dev.* **17**, 1646-1662.
Yamanaka, Y., Tamplin, O. J., Beckers, A., Gossler, A. and Rossant, J. (2007). Live imaging and genetic analysis of mouse notochord formation reveals regional morphogenetic mechanisms. *Dev. Cell* **13**, 884-896.